2020-09-09

Investigating the role of the c-Jun NH2-terminal kinase pathway in ErbB2-driven breast cancer and macrophage polarization

Lola Yu
University of Massachusetts Medical School

Investigating the role of the c-Jun NH_2-terminal kinase pathway in ErbB2-driven breast cancer and macrophage polarization

Lola Yu
Davis Lab
Master's Thesis
Cancer Biology Program

INTRODUCTION

Breast cancer is the second most common malignancy in the world, accounting for over 1.7 million new diagnoses and an estimated 500,000 deaths per year (1). Overexpression of the receptor tyrosine kinase ErbB2, also known as Her2 or Neu, occurs in over 30% of breast cancers and correlates with metastasis, poor prognosis, and decreased survival (1, 2). Although therapeutics targeting ErbB2 show clinical efficacy, many patients display no initial response or develop drug resistance over time (2). A deeper understanding of the molecular basis of ErbB2-driven tumorigenesis is thus required for the development of improved therapeutic strategies.

In vitro experiments suggest that activation of the c-Jun NH_2-terminal kinase (JNK) pathway, a mitogen-activated protein kinase pathway, promotes proliferation, cellular invasion, and stem cell expansion in ErbB2-driven breast cancer (3, 4). Furthermore, unpublished data from our lab using mammary epithelial cells expressing activated ErbB2 show that JNK is required for acinus formation in *in vitro* 3D cultures. In contrast to these studies showing a tumorigenic role for the JNK pathway, other data from our lab show that JNK loss results in accelerated breast tumor growth, suggesting a tumor suppressive role (5, 6). However, these studies were performed in p53 knockout mice with or without a Kras mutation, where the latter required extensive aging and genomic instability to occur before differences in tumor growth were observable. To date, limited *in vivo* studies exist to confirm the role of JNK in more biologically relevant breast tumor models, such as in ErbB2-mediated cancer, which accounts for over 30% of all human breast cancers. In addition, the molecular mechanisms by which JNK signaling promotes ErbB2-driven tumorigenesis remains poorly understood.

To address the discrepancy in JNK function between the *in vitro* ErbB2-driven breast cancer data and the *in vivo* p53 knockout tumor data, I began the development of an *in vivo* murine model to confirm the role of JNK in ErbB2-driven breast cancer. This mouse model will also allow us to test a potential mechanism by which JNK regulates tumorigenesis. Studies show that ErbB2-mediated secretion of the inflammatory cytokine IL6 promotes transformation and tumor growth by activation of the STAT3 transcription factor, triggering an IL6/STAT3 autocrine signaling loop (7,8). A major regulator of *Il6* gene expression includes activator protein 1 (AP-1), a transcription factor composed of downstream JNK targets in the Jun protein family (9). *In vitro* experiments using ErbB2-overexpressing mammary epithelial cell lines show that chemical inhibition of JNK suppresses secreted IL6 protein levels, supporting a role for the JNK pathway in IL6 regulation (7). Thus, I hypothesize that JNK drives ErbB2-driven breast cancer by promoting IL6-mediated tumor progression. Addressing this will increase our understanding of the role of JNK in ErbB2-driven breast cancer and reveal a potentially new mechanism by which JNK functions in tumor progression.

Additionally, I began the development of a mouse model that will allow us to investigate the role of JNK in macrophage polarization as an alternative mechanism by which JNK regulates ErbB2-driven breast cancer. In addition to promoting STAT3-dependent tumor growth, IL6 can indirectly drive tumorigenesis by promoting expression of the IL4 receptor in macrophages, triggering STAT6-mediated macrophage polarization towards the pro-tumorigenic M2 phenotype (10, 11). Unlike classically activated M1 macrophages, which promote inflammation and anti-tumor immunity, alternatively activated M2 macrophages function in immunosuppression and metastasis and correlate with advanced stages of breast cancer (12, 13). Further evidence supporting a role for the JNK pathway in macrophage polarization includes a recent study suggesting that JunB, a downstream JNK target and component of the AP-1 complex, plays a crucial role in the induction of M2 macrophage polarization in human alveolar macrophages (13). I hypothesize that activation of the JNK signaling pathway induces IL6-dependent macrophage polarization towards the pro-tumorigenic M2 phenotype. Addressing this hypothesis will determine for the first time whether JNK functions in regulating macrophage polarization within the tumor microenvironment, offering a potentially new mechanism by which JNK can promote ErbB2-driven breast cancer.

Determining the role of JNK in ErbB2-mediated breast cancer will have direct therapeutic relevance, as targeting JNK has the potential to inhibit ErbB2-driven breast cancer and other IL6-mediated diseases. Investigating the underlying mechanisms by which JNK functions in ErbB2-positive breast cancer can also offer new molecular targets and further contribute to effective drug design.

MATERIALS AND METHODS

Mice

The transgenic MMTV-NIC mouse model (JNK^{WT}) contains a transgene expressing the mouse mammary tumor virus long terminal repeat (MMTV-LTR) promoter, followed by a constitutively active form of ErbB2 (**N**eu), an internal ribosome entry site (**I**RES), and Cre recombinase (**C**re), or NIC (Figure 1a). The MMTV-LTR promoter ensures mammary cell-specific gene expression of ErbB2. The presence of an IRES site drives translation of *Cre* and ensures co-expression of *Neu* and *Cre* from the same bicistronic transcript. Due to the presence of Cre recombinase, this tumor mouse model can be crossed with any floxed transgenic mouse to induce mammary cell-specific deletion of a target-of-interest, such as *Jnk1/2* in this case. Once floxed *Jnk1/2* mice are successfully backcrossed to an FVB background, they will be crossed to the MMTV-NIC mouse model to induce mammary-specific deletion of *Jnk1/2*, generating a JNK^{KO} breast tumor model. To confirm the presence of the MMTV-NIC transgene in new litters, mice were genotyped by PCR analysis of genomic DNA to detect Cre recombinase. JNK^{WT} or MMTV-NIC mice were palpated weekly starting at 15 weeks of age. Tumors were measured using a caliper and mice were sacrificed once tumors reached 1 cm in diameter. MMTV-NIC mice were obtained from Dr. William J. Muller at McGill University.

NuTRAP mice were obtained from Dr. Evan Rosen at Beth Israel Deaconess Medical Center.

Backcrossing

To generate the JNK^{KO} (*Jnk1*$^{loxP/loxP}$*Jnk2*$^{loxP/loxP}$) MMTV-NIC tumor model, *Jnk1*$^{loxP/loxP}$*Jnk2*$^{loxP/loxP}$ C57BL/6J mice were first backcrossed to the FVB NJ background for five generations. *Jnk1*$^{loxP/+}$*Jnk2*$^{loxP/+}$ FVB NJ mice were then crossed to MMTV-NIC FVB NJ mice, getting one step closer to generating JNK^{KO} MMTV-NIC FVB NJ mice. (Future crosses will be performed and completed by other members of the lab.)

Backcrosses were performed by creating breeders with FVB NJ (male or female) mice with Bl/6 mice of a desired genetic background for five or more generations.

Analysis of tissue sections

Tissues from JNK^{WT} mice were fixed in 10% neutral buffer formalin for 18 hr, dehydrated, and embedded in paraffin. Tissue sections (7 um) were cut and stained with hematoxylin and eosin (H+E). The pathology of the tissues was then determined by Dr. David Garlick.

Primary Cell Line Generation

Breast tumors were dissected into DMEM/F12 media supplemented with 1% penicillin streptomycin and 2.4% nystatin (Sigma Aldrich, cat# N1638). Tumors were washed in phosphate-buffered saline and minced using a sterilized razor blade. Minced tumors were then digested in high glucose (4.5 g/L) DMEM media supplemented with 1% penicillin streptomycin and 2mg/mL collagenase (Sigma #C0130) for 2-3 hr rotating in 37˚C. Cells were centrifuged at 1000 RPM for 5 min and washed five times with 10 mL of PBS supplemented with 5% fetal bovine serum. Tumor cells were resuspended in

DMEM/F12 media supplemented with 2% FBS and 1% penicillin streptomycin. Cells were then plated on collagen I Rat Tail (Gibco Life Technologies, cat# A10483-01).

TRAP RNA Isolation

Dounce homogenization and RNA isolation of inguinal fat (100mg) from *Nutrap*$^{+/-}$ *Adipoq-Cre*$^{+}$ Bl/6 male mice, fed either a chow or high fat diet for 16 weeks, was performed as previously described by Roh et al (14). Tissues were dounce homogenized in 4 mL of homogenization buffer (50mM Tris, pH 7.5, 12mM $MgCl_2$, 100mM KCl, 1% NP-40, 100ug/ml cycloheximide, 1 mgl/ml sodium heparin, 2mM DTT, 0.2units/ul RNasin, 1x Complete EDTA-free protease inhibitor). Anti-GFP antibody (Abcam, cat# ab290) at 5ug/mL was used to pre-coat Protein G dynabeads (Life Technologies, cat# 10003D). The Qiagen Micro RNeasy kit (Qiagen, cat# 74004) was used following incubation of homogenates with dynabeads and samples were resuspended in diH_2O.

RNA Sequencing

Following TRAP RNA Isolation, RNA quality was determined using the Agilent Bioanalyzer and samples (at 1ug or greater) with a Rin value of 7 or higher were submitted for RNA sequencing to the BioMicro Center and samples were run on the NextSeq sequencer. RNA sequence analysis was performed by Yvonne Edwards (UMMS PMM Bioinformatics Core).

RESULTS

To define the role of JNK in ErbB2-driven breast cancer progression, I utilized the cre/loxP recombination system to begin the generation of ErbB2-driven breast cancer mouse models with either wild-type (JNK^{WT}) or JNK-deficient mammary cells (JNK^{KO}). To generate a control JNK^{WT} tumor model, the MMTV-NIC breast tumor mouse model, as described in Figure 1a, was crossed to wild-type FVB mice (*Jnk1*$^{+/+}$*Jnk2*$^{+/+}$). The MMTV-NIC or JNK^{WT} mouse model constitutively expresses *ErbB2* (or *Neu*) and results in spontaneous breast tumor formation (15, 16). To create an ErbB2-driven breast cancer mouse model with JNK-deficient mammary cells, MMTV-NIC mice will be crossed to mice expressing floxed *Jnk1* and *Jnk2* alleles (*Jnk1*$^{LoxP/LoxP}$*Jnk2*$^{LoxP/LoxP}$), as shown in Figure 1b. Because the JNK1 and JNK2 proteins display functional redundancy, deletion of both *Jnk1* and *Jnk2* genes is essential for understanding the role of the JNK pathway in tumor development (17).

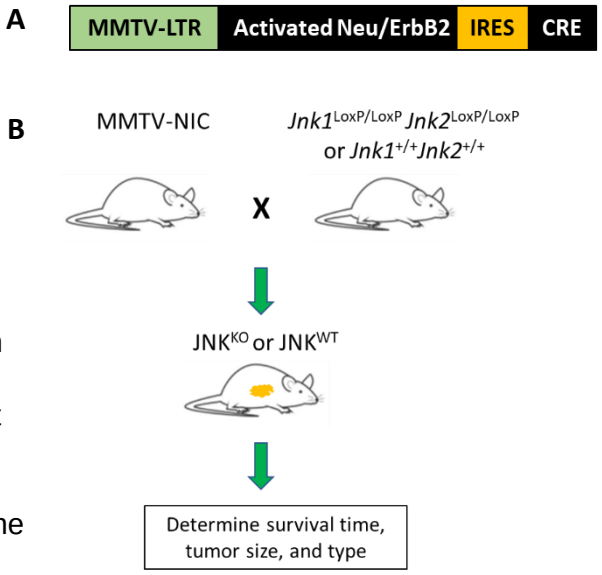

Figure 1. The MMTV-NIC breast tumor model and JNK^{KO} v JNK^{WT} breast tumor models. A) The transgenic MMTV-NIC mouse model expresses a constitutively active form of ErbB2 (**N**eu), an internal ribosome entry site (**I**RES), and Cre recombinase (**C**re). This NIC transgene is regulated by the mouse mammary tumor virus long terminal repeat (MMTV-LTR) promoter, which ensures mammary cell-specific gene expression. The presence of an IRES site drives translation of *Cre* and ensures co-expression of *Neu* and *Cre* from the same bicistronic transcript. **B)** General workflow and breeding scheme for JNK^{WT} and JNK^{KO} tumor models. +/+ indicates homozygous wild-type alleles. Yellow mass represents mammary tumor.

To date, I have confirmed that the JNK^{WT} (MMTV-NIC) model develops breast tumors in line with the published literature (15,16). JNK^{WT} mice developed palpable breast tumors at an average age of 138 days, similar to the published data of 146 days (n=8). The breast tumors from JNK^{WT} mice were characterized as multicentric mammary gland adenocarcinomas. The morphology of the tumors was consistent between JNK^{WT} mice having a nodular, solid pattern, a low mitotic index, and a fairly well

differentiated phenotype. In addition, 29% (2 out of 7) JNK^{WT} mice had lung metastases. Previous characterization of the MMTV-Neu model containing the same transgene as the MMTV-NIC model showed that 60% (3 out of 5) mice had lung metastases (16). The difference in the percentage of mice that develop lung metastases may be attributed to low mice numbers in both studies. Additionally, previous characterization of lung metastases was performed 30-60 days after tumors were first palpable. In this study, lungs were harvested once original tumors reached 1 cm in diameter or greater; from the time the tumors were first palpable to when tumors and lungs were harvested ranged from 7-22 days. Thus, it is possible that fewer mice had developed lung metastases in this study, given the earlier timepoint at which tumors and organs were harvested. Previous characterization had shown that in addition to the lungs, expression of the MMTV-NIC transgene was also upregulated in the salivary glands and to a lesser extent, in the pancreas (15,16). I therefore, also harvested salivary glands and pancreas to determine if any metastases had occurred in these tissues. Consistent with the published literature, no metastases were seen in the pancreas or salivary glands of the JNK^{WT} mice (15,16). Figure 2 shows representative images of breast tumors prior to dissection and H+E stained cross sections of breast tumors and lung metastases.

To generate JNK^{KO} mice, *Jnk1*$^{LoxP/LoxP}$*Jnk2*$^{LoxP/LoxP}$ mice had to first be backcrossed from a Bl/6 background to an FVB background, given that ErbB2-driven breast tumors do not develop spontaneously under a Bl/6 background (18). To date, I have successfully crossed *Jnk1*$^{LoxP/+}$*Jnk2*$^{LoxP/+}$ mice with FVB mice for five generations. I have also generated one breeder using a MMTV-NIC mouse and a *Jnk1*$^{LoxP/+}$*Jnk2*$^{LoxP/+}$ mouse under the FVB background. (Downstream generation of the JNK^{KO} mice will be performed by other members of the lab.) Once JNK^{KO} mice are successfully generated, tumor development and survival can be compared between JNK^{KO} and JNK^{WT} mice.

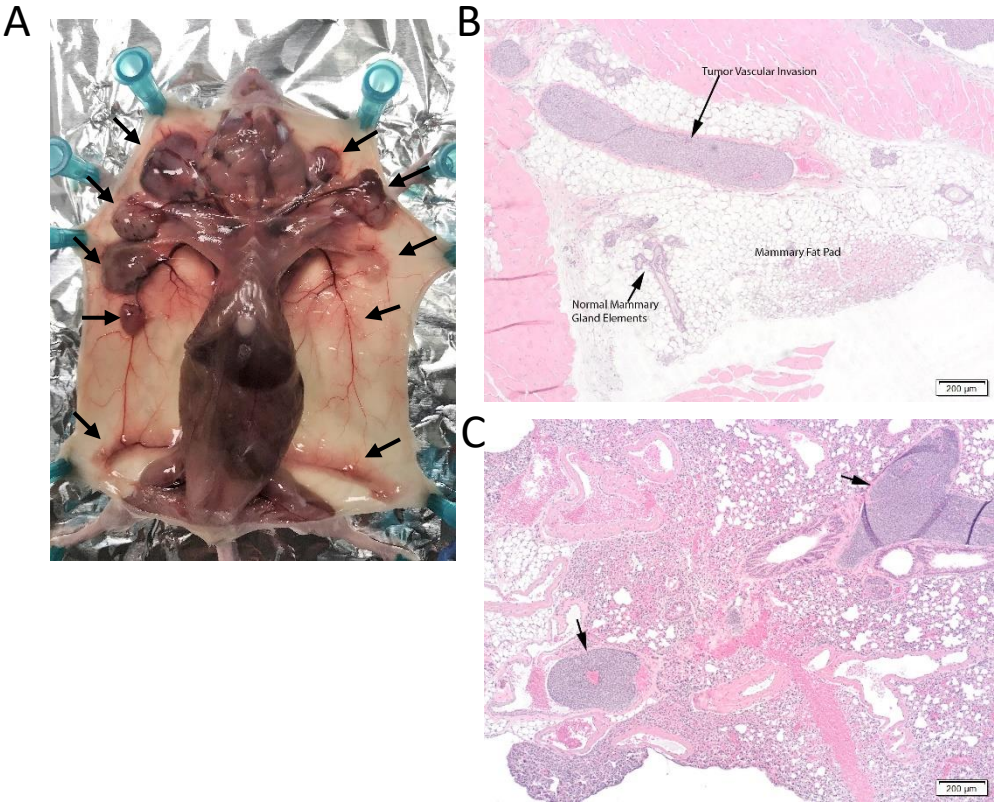

Figure 2. Representative images of JNK^{WT} (MMTV-NIC) mice. A) Image of JNK^{WT} mouse at 24 weeks-old. Breast tumors can arise from any of the 10 mammary glands (depicted by black arrows). Mice were taken down once any one of the tumors reached >1 cm in diameter as measured by caliper**. B)** Representative image of H+E stained 7um cross-section of a breast tumor from JNK^{WT} mouse, where normal mammary gland elements, the mammary fat pad, and tumor vascular invasion surrounding the tumor are marked. **C)** H+E stained 7um cross-section of lung tissue from a JNK^{WT} mouse, where lung metastases are marked by black arrows.

To determine whether JNK regulates ErbB2-driven proliferation by an IL6-dependent mechanism, IL6 RNA levels in the tumor cells of JNK^{WT} and JNK^{KO} mice can be compared (once the mouse models are fully developed). To allow for the downstream analysis of RNA expression in tumor cells specifically, I utilized the *Nutrap*$^{+/-}$ (Nuclear tagging and Translating

Ribosome Affinity Purification) mouse model developed by Dr. Evan Rosen (14). This mouse model allows for simultaneous isolation of mRNA and nuclei from any cell type in the presence of Cre recombinase. In the presence of Cre, a Stop codon is excised in the *Nutrap* transgene, allowing co-expression of the BirA biotin ligase, a biotin ligase recognition sequence (BLRP) fused to mCherry-RanGAP1 (a nuclear pore protein), and EGFP-L10a (a 60S ribosomal protein). BirA biotinylates the BLRP domain of the mCherry-RanGAP1 protein, allowing for easy downstream purification of biotin-labeled nuclei and subsequent DNA sequencing; EGFP-L10a allows for the affinity purification of ribosomes and hence, isolation of actively-translating RNA and downstream RNA sequencing. Crossing the *Nutrap*$^{+/-}$ mice to the JNK^{KO} and JNK^{WT} mice will allow for ribosome-labeling of only mammary cells and hence, downstream mRNA sequencing of specifically breast tumor cells.

In order to utilize the *Nutrap*$^{+/-}$ mice in an ErbB2-driven breast cancer mouse model, I had to first backcross the mice from a Bl/6 background to an FVB background. To date, I have successfully backcrossed the *Nutrap*$^{+/-}$ mice up to 5 generations under the FVB background. These mice are now available to be crossed to the JNK^{WT} and JNK^{KO} mice.

As a proof-of-concept experiment to demonstrate that the TRAP RNA isolation works as previously described, I performed TRAP RNA isolation on the inguinal fat of *Nutrap*$^{+/-}$ *Adipoq-Cre*$^{+}$ Bl/6 male mice fed either a chow diet or high fat diet for 16 weeks. For unknown reasons, E. coli contamination was present in the chow diet group, which may have been due to contaminations from other samples, as sequencing was run with multiple samples per lane. There was lower than expected read mapping rates to the mouse reference, with 32-42% mapping in the chow diet group and 72-77% mapping in the high fat diet group. Despite this, differentially expressed genes were determined, as shown in Table 1, although this experiment should be repeated for further validation.

To test whether JNK in ErbB2-driven breast cancer plays a role in macrophage polarization, tumors from JNK^{WT} and JNK^{KO} mice (once models are fully developed) can be harvested and flow cytometry can be used to determine the population sizes of M1 and M2 macrophages by gating on M1 markers, such as CD38, Gpr18, and Fpr2, and M2 markers, including Egr2 and c-Myc (19). Macrophage

Table 1. Pathway enrichment. Differentially expressed genes between chow diet and high fat diet groups (q<0.05; |log2FC| >1) N=982. C= # of reference genes in category; O = # of genes in user gene and also in category; FDR = false discovery rate

KEGG PATHWAY	C	O	FDR	OverlapGene_UserID
Metabolism of xenobiotics by cytochrome P450	65	13	0.0012	Gstt3; Cyp2f2; Gstm1; Gstt1; Ugt1a2; Ugt1a10; Ugt1a7c; Ugt1a5; Ugt1a9; Ugt1a6b; Ugt1a1; Mgst3; Ugt1a6a
Porphyrin and chlorophyll metabolism	41	10	0.0012	Hmox1; Alad; Ugt1a2; Ugt1a10; Ugt1a7c; Ugt1a5; Ugt1a9; Ugt1a6b; Ugt1a1; Ugt1a6a
Ascorbate and aldarate metabolism	27	8	0.0014	Ugt1a2; Ugt1a10; Ugt1a7c; Ugt1a5; Ugt1a9; Ugt1a6b; Ugt1a1; Ugt1a6a
Drug metabolism - cytochrome P450	67	12	0.0023	Gstt3; Gstm1; Gstt1; Ugt1a2; Ugt1a10; Ugt1a7c; Ugt1a5; Ugt1a9; Ugt1a6b; Ugt1a1; Mgst3; Ugt1a6a
Pentose and glucuronate interconversions	34	8	0.0054	Ugt1a2; Ugt1a10; Ugt1a7c; Ugt1a5; Ugt1a9; Ugt1a6b; Ugt1a1; Ugt1a6a
Non-alcoholic fatty liver disease (NAFLD)	153	18	0.0067	Cebpa; Cox7a2; Cox8a; Eif2s1; Eif2ak3; Insr; Lep; Ndufa4; Prkag1; Ndufs8; Ndufs5; Ndufa3; Ndufc1; Uqcrh; Uqcrc2; Ndufa5; Ndufb10; Ndufab1
Oxidative phosphorylation	134	16	0.0114	Atp5j; Atp6v0e; Cox7a2; Cox8a; Ndufa4; Ndufs8; Tcirg1; Ndufs5; Ndufa3; Ndufc1; Uqcrh; Uqcrc2; Ndufa5; Ndufb10; Ndufab1; Atp6v0e2
Drug metabolism - other enzymes	51	9	0.0117	Ces1e; Ugt1a2; Ugt1a10; Ugt1a7c; Ugt1a5; Ugt1a9; Ugt1a6b; Ugt1a1; Ugt1a6a
Huntington's disease	194	20	0.0117	Atp5j; Cox7a2; Cox8a; Ndufa4; Pparg; Ucp1; Ndufs8; Ap2s1; Polr2h; Ndufs5; Ndufa3; Ndufc1; Polr2l; Uqcrh; Uqcrc2; Dctn4; Ndufa5; Ndufb10; Ndufab1; Ift57
Proteasome	45	8	0.0210	Psma2; Psmb10; Psmb4; Psmd4; Psme2; Shfm1; Psmb2; Psme2b
Chemical carcinogenesis	93	12	0.0210	Gstt3; Gstm1; Gstt1; Ugt1a2; Ugt1a10; Ugt1a7c; Ugt1a5; Ugt1a9; Ugt1a6b; Ugt1a1; Mgst3; Ugt1a6a

phenotypes can be further characterized by sorting M1 and M2 populations by FACS and using qPCR to measure expression levels of known M1 macrophage-associated genes, including *Cd11c, Il1β, Nos1, Tnfα*, and M2 macrophage-associated genes *Mgl1, Mrc1, Ccl17, and Ccl22* (20).

DISCUSSION

Generating the JNK^{WT} and JNK^{KO} mice as described here, will allow us to determine the role of the JNK pathway in ErbB2-driven breast cancer. To date, I have validated the JNK^{WT} mice and have shown that the tumor characteristics are similar to those previously published. The JNK^{KO} mice are currently being generated, where *Jnk1*$^{LoxP/+}$*Jnk2*$^{LoxP/+}$ mice have been successfully backcrossed five generations into an FVB background and are undergoing crosses with MMTV-NIC mice. Once JNK^{KO} mice are generated, tumor progression and tumor characteristics of the JNK^{WT} and JNK^{KO} mice can be compared to determine the role of JNK in ErbB2-driven breast cancer and any differences in macrophage polarization can also be determined.

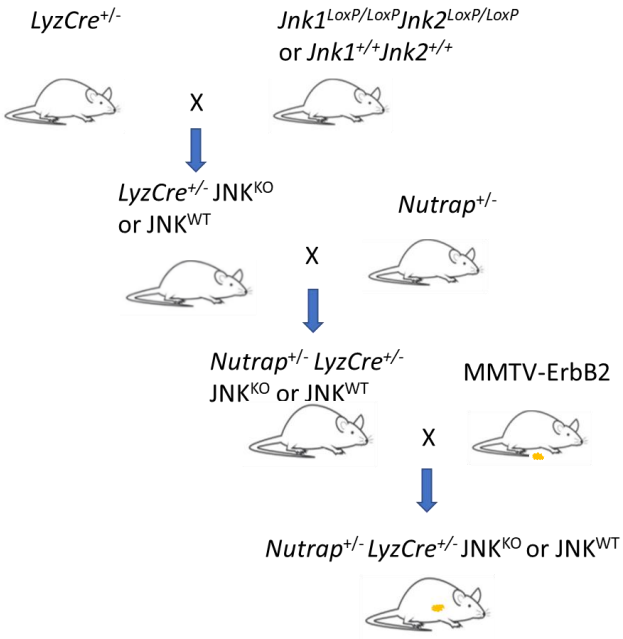

Figure 3. Generation of a mouse model to test the role of macrophage-specific JNK in ErbB2-driven breast cancer progression and survival.

The upstream JNK regulators, MKK4 and MAP3K1, are frequently mutated in various forms of breast cancer; however, JNK mutations are not as commonly found (21, 22, 23). Because MKK4 and MAP3K1 may regulate other downstream proteins besides JNK that function in tumorigenesis, JNK deletion alone may not completely abrogate tumor growth. Thus, I believe that the JNK^{KO} mice described in this study will delay tumor progression but may not result in complete tumor abrogation.

In this study, I have also backcrossed *Nutrap*$^{+/-}$ mice for five generations into an FVB background. Once JNK^{KO} mice are available, *Nutrap*$^{+/-}$ mice can be crossed with both JNK^{KO} and JNK^{WT} mice and allow for easy RNA isolation of tumor cells and downstream RNA sequencing. This will allow us to determine whether the JNK pathway functions through an IL6-dependent mechanism, while also giving us a comprehensive analysis of differences in actively-translating RNA, which may reveal other previously unknown mechanisms by which JNK functions in ErbB2-driven breast cancer. I believe that in addition to augmentations in the IL-6 pathway, JNK deletion will also result in changes in other inflammatory cytokines regulated by JNK, such as IL-1 and TNFa. Changes in the expression of apoptosis regulators is also likely, as downstream targets of JNK also include BIM, BAD, Mcl1, and the Bcl2 family of proteins (17, 24).

In addition to the questions proposed in this work, another underlying problem that remains unaddressed is which cell type JNK plays the greatest role in during breast cancer progression. To date, a direct and rigorous comparison of the role of JNK in tumor cells, versus macrophages, has not been performed. To determine the role of JNK in macrophages, as opposed to tumor cells, during ErbB2-driven breast cancer, a *LyzCre*$^{+/-}$ *Nutrap*$^{+/-}$ JNK^{WT} and JNK^{KO} tumor mouse model can be generated (Figure 3). To do this, *LyzCre*$^{+/-}$ mice have to first be backcrossed from a Bl/6 background to an FVB background. To date, I have crossed the *LyzCre*$^{+/-}$ mice to FVB mice for four generations, and the mice require one more FVB cross before they can be used to generate a breast tumor model. Although addition of the *Nutrap* gene is not necessary to determine the role of JNK in macrophages on ErbB2-

induced tumor progression, its presence allows for downstream RNA and DNA analysis of tumor-associated macrophages in JNK^{KO} and JNK^{WT} mice. Once these mice are generated, tumor progression and survival can be compared between tumor-specific JNK^{KO} mice and macrophage-specific JNK^{KO} mice. Because JNK has been shown to also play a major role in IL6 regulation in macrophages and macrophage polarization, I believe that JNK functions in both tumor cells, as well as tumor-associated macrophages, to promote tumor progression in ErbB2-driven breast cancer (20). Defining the role of JNK in tumor cells as compared to macrophages will better inform us on which cell type to target for therapeutic purposes.

In addition to the *Jnk1*$^{LoxP/+}$*Jnk2*$^{LoxP/+}$, *Nutrap*$^{+/-}$, and *LyzCre*$^{+/-}$ mice, I have also started Bl/6-to-FVB backcrosses of *Il6*$^{LoxP/LoxP}$, *Mkk4*$^{+/-}$, and *Mkk7*$^{+/-}$ mice for future experiments to determine the role of these other JNK pathway proteins on breast cancer progression. Because mutations in MKK4 and MKK7 are seen more frequently in breast cancer than JNK mutations, I hypothesize that deletion of MKK4 and MKK7 will result in a greater delay of tumor progression than JNK deletion (21, 22, 23). Because IL-6 expression can be induced through JNK-independent mechanisms, such as through p38 pathway activation, I believe that *Il6* deletion in the ErbB2 mouse model will inhibit tumor growth to a greater extent than JNK deletion.

Lastly, I would like to address my thoughts on the varying, and sometimes contradicting roles of JNK seen in different cellular contexts. I believe that the varying functions of the JNK pathway in different cancer models can be attributed, in part, by differences in JNK isoform-specific functions. It is important to note that there are three genes: *jnk1*, *jnk2*, and *jnk3*, which can encode a total of ten different isoforms of JNK proteins (25). Previous data have shown that different JNK isoforms have varying and opposing functions. For example, experiments in colon cancer reveal that knockdown of JNK1α1 leads to increased cell death, whereas knockdown of JNK1α2 and JNK1β2 causes decreased apoptosis (26). To define the role of individual JNK isoforms, future experiments targeting isoform-specific exons in the three JNK genes can be performed to selectively knock-out specific JNK isoforms in tumor models.

Furthermore, I believe that JNK isoforms have distinct functions because of differences in their substrate binding preferences. Support for this hypothesis comes from previous studies showing that all ten isoforms differ in their binding to ATF-2, c-Jun, and Elk-1 transcription factors (25). However, JNK isoform-specific substrates remain uncharacterized. Further studies must be conducted to determine the substrates of specific JNK isoforms. In the future, it will be important to determine any differences in JNK isoform expression between breast cancer models, as JNK isoforms can have varying downstream targets, which may contribute to the opposing biological outcomes of JNK deletion seen in past studies. Because JNK proteins are expressed in multiple tissue types and serve various biological functions, defining the distinct functions and substrates of individual isoforms will be imperative in the therapeutic targeting of the JNK pathway in cancer.

Additionally, it is possible that the discrepancy in the function of JNK in various cancer types is caused, not by the mere presence or absence of JNK, but by JNK protein dynamics. Changes in JNK dynamics, defined as the duration of activation, leads to opposing downstream effects in fibroblasts and T cells. Chronic JNK stimulation in T cells and fibroblasts results in apoptosis, which directly opposes the cell survival effects of transient JNK activation (27, 28). To determine whether JNK dynamics play a role in breast cancer development, we can induce acute inhibition of JNK in the ErbB2 breast cancer mouse model by injection of a JNK inhibitor for several timepoints throughout tumor development; overall survival and tumor development from this model can be compared to chronic JNK deletion as present in the JNK^{KO} model described in this work. Future studies will be required to determine how differences in the dynamics of JNK expression affect varying cancer models. If distinct JNK protein dynamics in fact define the downstream biological effect, it is possible to use these differences in protein dynamics as a screening tool to understand whether cancer patients will benefit from JNK inhibition or JNK activation.

REFERENCES

1. Slamon DJ, Godolphin W, Jones LA, Holt JA, Wong SG, Keith DE, Levin WJ, Stuart SG, Udove J, Ullrich A, et al. Studies of the HER-2/neu proto-oncogene in human breast and ovarian cancer. Science. 1989;244(4905):707-12. PubMed PMID: 2470152.
2. Tan M, Yu D. Molecular mechanisms of erbB2-mediated breast cancer chemoresistance. Adv Exp Med Biol. 2007;608:119-29. PubMed PMID: 17993237.
3. Guo W, Pylayeva Y, Pepe A, Yoshioka T, Muller WJ, Inghirami G, Giancotti FG. Beta 4 integrin amplifies ErbB2 signaling to promote mammary tumorigenesis. Cell. 2006;126(3):489-502. doi: 10.1016/j.cell.2006.05.047. PubMed PMID: 16901783.
4. Jiao X, Katiyar S, Willmarth NE, Liu M, Ma X, Flomenberg N, Lisanti MP, Pestell RG. c-Jun induces mammary epithelial cellular invasion and breast cancer stem cell expansion. J Biol Chem. 2010;285(11):8218-26. doi: 10.1074/jbc.M110.100792. PubMed PMID: 20053993; PMCID: PMC2832973.
5. Cellurale, C., Girnius, N., Jiang, F., Cavanagh-Kyros, J., Lu, S., Garlick, D. S., Mercurio, A. M., Davis, R. J. Role of JNK in Mammary Gland Development and Breast Cancer. Cancer Research. 2011; *72*(2), 472–481. doi: 10.1158/0008-5472.can-11-1628. PubMed PMID: 22127926 PMCID: PMC3261359.
6. Girnius, N., Edwards, Y. J. K., Garlick, D. S., & Davis, R. J. The cJUN NH2-terminal kinase (JNK) signaling pathway promotes genome stability and prevents tumor initiation. *ELife*. 2018; *7*, 1–25. doi: 10.7554/elife.36389; PubMed PMID: 29856313; PMCID: PMC5984035.
7. Hartman ZC, Yang XY, Glass O, Lei G, Osada T, Dave SS, Morse MA, Clay TM, Lyerly HK. HER2 overexpression elicits a proinflammatory IL-6 autocrine signaling loop that is critical for tumorigenesis. Cancer Res. 2011;71(13):4380-91. doi: 10.1158/0008-5472.CAN-11-0308. PubMed PMID: 21518778; PMCID: PMC3129398.
8. Rodriguez-Barrueco R, Yu J, Saucedo-Cuevas LP, Olivan M, Llobet-Navas D, Putcha P, Castro V, Murga-Penas EM, Collazo-Lorduy A, Castillo-Martin M, Alvarez M, Cordon-Cardo C, Kalinsky K, Maurer M, Califano A, Silva JM. Inhibition of the autocrine IL-6-JAK2-STAT3-calprotectin axis as targeted therapy for HR-/HER2+ breast cancers. Genes Dev. 2015;29(15):1631-48. doi: 10.1101/gad.262642.115. PubMed PMID: 26227964; PMCID: PMC4536311.
9. Ndlovu MN, Van Lint C, Van Wesemael K, Callebert P, Chalbos D, Haegeman G, Vanden Berghe W. Hyperactivated NF-{kappa}B and AP-1 transcription factors promote highly accessible chromatin and constitutive transcription across the interleukin-6 gene promoter in metastatic breast cancer cells. Mol Cell Biol. 2009;29(20):5488-504. doi: 10.1128/MCB.01657-08. PubMed PMID: 19687301; PMCID: PMC2756884.
10. Mauer J, Denson JL, Bruning JC. Versatile functions for IL-6 in metabolism and cancer. Trends Immunol. 2015;36(2):92-101. doi: 10.1016/j.it.2014.12.008. PubMed PMID: 25616716.
11. Chanmee T, Ontong P, Konno K, Itano N. Tumor-associated macrophages as major players in the tumor microenvironment. Cancers (Basel). 2014;6(3):1670-90. doi: 10.3390/cancers6031670. PubMed PMID: 25125485; PMCID: PMC4190561.
12. Linde N, Casanova-Acebes M, Sosa MS, Mortha A, Rahman A, Farias E, Harper K, Tardio E, Reyes Torres I, Jones J, Condeelis J, Merad M, Aguirre-Ghiso JA. Macrophages orchestrate breast cancer early dissemination and metastasis. Nat Commun. 2018;9(1):21. doi: 10.1038/s41467-017-02481-5. PubMed PMID: 29295986; PMCID: PMC5750231.
13. Xue J, Schmidt SV, Sander J, Draffehn A, Krebs W, Quester I, De Nardo D, Gohel TD, Emde M, Schmidleithner L, Ganesan H, Nino-Castro A, Mallmann MR, Labzin L, Theis H, Kraut M, Beyer M, Latz E, Freeman TC, Ulas T, Schultze JL. Transcriptome-based network analysis reveals a spectrum model of human macrophage activation. Immunity. 2014;40(2):274-88. doi: 10.1016/j.immuni.2014.01.006. PubMed PMID: 24530056; PMCID: PMC3991396.
14. Roh HC, Tsai L, Lyubetskaya A, Tenen D, Kumari M, Rosen ED. Simultaneous transcriptional and epigenomic profiling from specific cell types within heterogeneous tissues in vivo. Cell

Rep. 2017;18(4):1-48-1061. doi: 10.1016/j.celrep.2016.12.087. PubMed PMID: 28122230; PMCID: PMC5291126.
15. Ursini-Siegel J, Hardy WR, Zuo D, Lam SH, Sanguin-Gendreau V, Cardiff RD, Pawson T, Muller WJ. ShcA signalling is essential for tumour progression in mouse models of human breast cancer. EMBO J. 2008;27(6):910-20. doi: 10.1038/emboj.2008.22. PubMed PMID: 18273058; PMCID: PMC2274931.
16. Siegel PM, Ryan ED, Cardiff RD, Muller WJ. Elevated expression of activated forms of Neu/ErbB-2 and ErbB-3 are involved in the induction of mammary tumors in transgenic mice: implications for human breast cancer. EMBO J. 1999;18(8):2149-64. doi: 10.1093/emboj/18.8.2149. PubMed PMID: 10205169; PMCID: PMC1171299.
17. Tournier C, Hess P, Yang DD, Xu J, Turner TK, Nimnual A, Bar-Sagi D, Jones SN, Flavell RA, Davis RJ. Requirement of JNK for stress-induced activation of the cytochrome c-mediated death pathway. Science. 2000;288(5467):870-4. doi. 10.1126/science.288.5467.870. PubMed PMID: 10797012.
18. Fry, E. A., Taneja, P., & Inoue, K. Clinical applications of mouse models for breast cancer engaging HER2/neu. Integrative Cancer Science and Therapeutics. 2016; *3*(5). doi:10.15761/icst.1000210. PubMed PMID: 28133539; PMCID: PMC5267336.
19. Jablonski, K. A., Amici, S. A., Webb, L. M., Ruiz-Rosado, J.D., Popovich, P. G., Partida-Sanchez, S., Guerau-de-Arellano, M. Novel Markers to Delineate Murine M1 and M2 Macrophages. PLOS ONE. 2015; *10*(12), e0145342. doi: 10.1371/journal.pone.0145342. Pubmed PMID: 2669961; PMCID: PMC4689374.
20. Han MS, Jung DY, Morel C, Lakhani SA, Kim JK, Flavell RA, Davis RJ. JNK expression by macrophages promotes obesity-induced insulin resistance and inflammation. Science. 2013; 339(6116):218-22. doi: 10.1126/science.1227568. PubMed PMID: 23223452; PMCID: PMC3835653.
21. Cancer Genome Atlas N. Comprehensive molecular portraits of human breast tumours. Nature. 2012; 490: 61-70. doi. 10.1038/nature11412. PubMed PMID: 23000897; PMCID: PMC3465532.
22. Stephens PJ, Tarpey PS, Davies H, Van Loo P, Greenman C, Wedge DC, Nik-Zainal S, Martin S, Varela I, Bignell GR et al. The landscape of cancer genes and mutational processes in breast cancer. Nature. 2012; 486: 400-404. doi: 10.1038/nature11017. PubMed PMID: 22722201; PMCID: PMC3428862.
23. Nik-Zainal S, Davies H, Staaf J, Ramakrishna M, Glodzik D, Zou X, Martincorena I, Alexandrov LB, Martin S, Wedge DC et al. Landscape of somatic mutations in 560 breast cancer whole-genome sequences. Nature. 2016; 534: 47-54. doi: 10.1038/nature17676. PubMed PMID: 27135926; PMCID: PMC4910866.
24. Xia Z, Dickens M, Raingeaud J, Davis RJ, Greenberg ME. Opposing effects of ERK and JNK-p38 MAP kinases on apoptosis. Science. 1995; 270: 1326-1331. doi. 10.1126/science.270.5240.1326. PubMed PMID: 7481820.
25. Gupta S, Barrett T, Whitmarsh AJ, Cavanagh J, Sluss HK, Dérijard B, Davis RJ. Selective interaction of JNK protein kinase isoforms with transcription factors. The EMBO Journal. 1996; 15(11): 2760. PubMed PMID: 8654373; PMCID: PMC450211.
26. Mahalingam D, Keane M, Pirianov G, Mehmet H, Samali A, Szegezdi E. Differential activation of JNK1 isoforms by TRAIL receptors modulate apoptosis of colon cancer cell lines. British Journal of Cancer. 2009; 100(9): 1415. doi: 10.1038/sj.bjc.6605021. PubMed PMID: 19352384; PMCID: PMC2694422.
27. Lamb JA, Ventura J, Hess P, Flavell RA, Davis RJ. JunD mediates survival signaling by the JNK signal transduction pathway. Molecular Cell. 2003; 11(6): 1479. doi. 10.1016/s1097-2765(03)00203-x. PMID: 12820962.
28. Chen Y, Wang X, Templeton D, Davis RJ, Tan T. The role of c-jun N-terminal kinase (JNK) in apoptosis induced by ultraviolet C and gamma radiation. duration of JNK activation may determine cell death and proliferation. The Journal of Biological Chemistry. 1996; 271(50): 31929. doi: 10.1074/jbc.271.50.31929. PMID: 8943238.